Journal of Superconductivity and Novel Magnetism (2026) 39:56
https://doi.org/10.1007/s10948-026-07147-2

RESEARCH

Dynamic Study of the Environmental Impact on Gap Relaxation Time in NbTi Superconducting Wire

K. Harrabi[1,2]

Received: 27 September 2025 / Accepted: 8 February 2026

Abstract
We have studied non-equilibrium states in NbTi films deposited on fused silica under different surrounding conditions using electrical current pulses. When the applied current exceeds the depairing current I_c, a voltage response is observed after a characteristic delay time t_d. Although the sample dimensions are much larger than the coherence length ξ, the localized micro-metric region formed corresponds to a hotspot. The delay times are quantitatively described using the Time-Dependent Ginzburg–Landau (TDGL) theory of M. Tinkham, enabling the determination of filament cooling times for the same sample in both liquid helium and vacuum. We find cooling times of about $\tau_d = 6.0 \pm 0.5$ ns in vacuum and 5.3 ± 0.5 ns in liquid helium. These results demonstrate that liquid helium has only a minor effect on the film cooling time, with most of the heat being transferred into the substrate via phonons.

Keywords Hotspot · Non-equilibrium · Superconductivity · Critical currnet

1 Introduction

The formation of non-equilibrium states in quasi-one-dimensional and two-dimensional superconducting filaments has been the subject of extensive theoretical and experimental research in recent years [1–4]. These systems are particularly interesting because they combine reduced dimensionality with the intrinsic quantum nature of superconductivity, giving rise to rich non-equilibrium dynamics. Among the most widely studied phenomena are the emergence of resistive states, which represent local breakdowns of superconductivity under strong excitation. Such resistive states not only provide fundamental insights into superconducting dynamics, but also play a crucial role in practical applications of nanoscale superconducting devices.

Over the past decade, the deliberate creation and control of resistive states in superconducting nanowires have proven to be a powerful tool for applications in superconducting nano-circuitry [5, 6]. One of the most fascinating directions is their use in highly sensitive infrared detectors [7, 8] and in the field of quantum information, particularly in superconducting qubits [9, 10]. The utility of such devices relies on the extraordinary sensitivity of superconducting filaments to external excitations, which can trigger a transition from the superconducting state to a resistive one. In superconducting nanowire single-photon detectors (SNSPDs), for example, the detection mechanism is based on the localized suppression of superconductivity upon photon absorption. This suppressed region, commonly referred to as a hotspot, acts as the nucleus of a resistive domain. The formation and dynamical evolution of the hotspot are decisive factors in detector performance, directly influencing detection sensitivity, timing jitter, and reset time.

The physics of hotspot dynamics is closely tied to energy dissipation in the superconducting state. Once a hotspot is formed, energy is released as the system transitions locally to the normal state. This energy is carried predominantly by quasiparticles and phonons, and its spatial propagation and redistribution determine how quickly the superconducting wire recovers. Ultimately, the heat generated in the wire must be evacuated into the substrate in the form of phonons. The efficiency of this process depends strongly on the thermal boundary conductance between the superconducting film and its surrounding environment. Consequently, both the substrate material and the external medium, such as liquid helium or

✉ K. Harrabi
harrabi@kfupm.edu.sa

[1] Physics Department, King Fahd University of Petroleum and Minerals, Dhahran 31261, Saudi Arabia

[2] Interdisciplinary Research Center (RC) for Advanced Quantum Computing, KFUPM, Dhahran 31261, Saudi Arabia

Published online: 05 March 2026

vacuum, play significant roles in the relaxation process. Understanding how these parameters affect heat transfer is essential for optimizing the performance of superconducting devices that rely on rapid recovery from non-equilibrium states.

In the present work, we investigate the creation of non-equilibrium states in NbTi superconducting filaments induced by electrical current pulses under different environmental conditions. When the applied current exceeds the depairing current I_c, a dissipative normal zone develops after a characteristic delay time t_d [11]. This delay provides a direct window into the timescales of non-equilibrium dynamics in superconducting wires. By analyzing the dependence of t_d on the magnitude of the overcritical current, and fitting the results with TDGL proposed by Tinkham [12], we extract the phonon escape times in different environments.

Our measurements reveal a systematic difference between samples studied in vacuum and those immersed in liquid helium. Specifically, we find that the heat escape time is slightly shorter in liquid helium than in vacuum, though the effect is minor. This observation indicates that most of the heat is dissipated into the substrate rather than into the external medium. The results highlight the central role of the film-substrate interface in governing non-equilibrium heat transfer, while showing that the surrounding liquid helium contributes only marginally to cooling. These findings provide new insight into the microscopic processes controlling energy relaxation in superconducting nanostructures and may help guide the design of next-generation superconducting detectors and quantum devices with improved performance.

2 Experimental Setup

NbTi filaments, 50 nm thick and 5 μm wide, were deposited on fused silica substrates by DC magnetron sputtering under high-vacuum conditions. The superconducting filaments and gold contacts were defined using standard photolithographic techniques followed by ion milling. The sample geometry is shown in Fig. 1: the central section contains a constriction with a length of 600 μm. Current pulses were applied through the wire and directed to ground, while two wide superconducting side probes were integrated into the layout to measure the voltage drop across the filament.

For measurements in vacuum, a closed-cycle cryostat was employed to reach a base temperature of 4 K. The same sample was subsequently immersed in a liquid helium dewar and tested using the identical setup. Current pulses of variable amplitude, with a duration of 450 ns and a repetition rate of 10 kHz, were applied through an air-delay line of 240 ns [13]. The resulting voltage response was monitored with a high-speed oscilloscope. Current pulses were applied through the wire and directed to ground, while two wide superconducting side probes were integrated into the layout to measure the voltage drop across the filament. The current flowing in the sample was determined by $I = 2V/50$, where V is the applied voltage. The superconducting transition temperature of the films was approximately 7.8 K. All samples fabricated from the same substrate patch showed consistent behavior, with the hotspot forming reproducibly near the central region between the two electrodes, indicating good film uniformity.

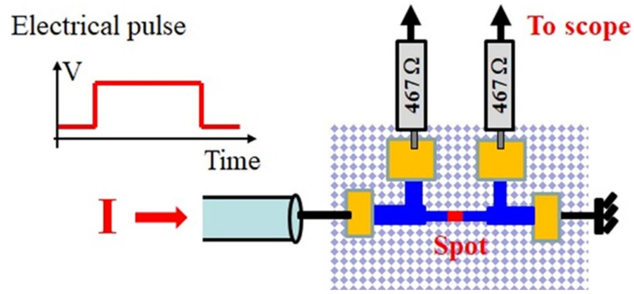

Fig. 1 Schematic of the sample layout showing the narrow NbTi filament and two lateral voltage probes connected to the oscilloscope through 467 resistors. The current pulse is applied along the wire and directed to ground. The formation of a resistive region within the narrow filament is anticipated from the device geometry, and its localization between the two probes is inferred from probe-resolved voltage measurements, as discussed in the text

3 Experimental Results and Discussion

3.1 Dissipation of Non-Equilibrium States

When a supercritical current is abruptly applied to a superconducting filament, the resistive voltage does not appear immediately. During this initial transient, quasiparticles and phonons are driven out of equilibrium, while superconductivity can temporarily persist even though the applied current exceeds I_c, resulting in a measurable delay before a voltage develops. At later times, this transient non-equilibrium superconducting state may evolve into a localized dissipative non-equilibrium region, where superconductivity breaks down and a resistive response emerges.

Under these conditions, superconductivity breaks down locally and energy dissipation appears. Several distinct modes have been identified as being responsible for such metastable states, most prominently the phase slip center (PSC) and the hotspot (HS)[11]. Both of these dissipation modes are of fundamental importance in the study of non-equilibrium superconductivity and have also been employed as powerful tools in particle detection and photon-sensing technologies. For a superconducting wire biased with a current close to the pair-breaking current, dissipation can additionally be initiated by the motion of vortices, which may be induced either by an external magnetic field or by the self-field of the applied current.

Phase slip centers were first observed in one-dimensional superconducting whiskers, where the width of the conductor is comparable to the coherence length ξ. When the applied current increases, the Cooper pairs accelerate until the critical velocity is reached. At this point, the pairs break within a region of size ξ, producing a localized zone where the order parameter collapses to zero and superconductivity vanishes. In this region, the normal electrons diffuse almost instantaneously, and across its boundaries the phase of the superconducting wave function undergoes a discontinuous slip by 2π. This process is interpreted as an oscillation of the order parameter between zero and one in the time domain. During such events, both the normal electrons and the remaining Cooper pairs contribute to the overall current transport [15].

When the transverse size of the superconducting wire is much larger than ξ, dissipation is instead governed by phase slip lines (PSLs), which exhibit behavior analogous to PSCs but on a wider spatial scale. PSLs can be explained as transverse flows involving a vortex and an antivortex moving in opposite directions and annihilating at the center of the filament [16, 17]. The dynamics of these structures have been extensively investigated within the theoretical framework of the TDGL [18, 19]. Although PSCs and PSLs differ in their microscopic physical realization, they manifest in similar macroscopic transport features. In particular, both mechanisms produce steps and voltage jumps in the current-voltage characteristics [20]. Remarkably, the linear portions of these voltage steps converge toward a single point, which is referred to as the superconducting current [21].

3.2 Measurement of the Heat Escape Time

Dissipative states induced by an electrical current pulse are generated in superconducting wires once the applied current exceeds the critical current I_c. Although in wide superconducting strips edge-enhanced current density and vortex-mediated dissipation are often expected, no distinct voltage features that could be uniquely attributed to vortex motion were identified prior to the appearance of the delayed voltage response in the present measurements. However, we note that flux-flow dissipation does not necessarily require pre-onset voltage jumps or fluctuations and may result in a smooth voltage increase once dissipation sets in. Therefore, while the observed behavior is consistent with hotspot-related dissipation, the possible contribution of vortex motion to the emerging resistance cannot be excluded. The delay time t_d represents the characteristic time required for the collapse of superconductivity in the affected region.

Ref. [14] reported a detailed investigation of the dissipative mechanisms preceding the onset of the delay time t_d, and examined the influence of an external magnetic field on this process. In that work, the collapse of superconductivity in a two-dimensional filament was associated with the nucleation of vortices and the subsequent formation of phase slip lines (PSLs). Interestingly, it was shown that the delay time becomes independent of temperature in the quasi-equilibrium limit, in contrast to models where the delay time is governed by non-equilibrium quasiparticle or vortex-related dynamics rather than by thermal relaxation, and is therefore expected to exhibit a strong temperature dependence for different ratios of I_c.

Hotspot localization in the present devices is primarily determined by the lithographically defined constriction, which produces a maximum current density at the central region of the filament, as established in previous theoretical and experimental studies. Although spatially resolved mapping of the local critical current was not performed, the reproducible electrical response observed across multiple samples indicates consistent nucleation of the dissipative region near the center of the wire. No experimental signatures typically associated with vortex motion, such as pre-onset voltage steps or fluctuations prior to the delay time td, were observed, even for measurements performed close to Tc. These observations suggest that the dissipation mechanism in the present NbTi films is dominated by hotspot formation." In our experiment, no evidence of the phenomena described in Ref. [14] was observed. In particular, we did not detect signatures of quasi-particle avalanches or vortex flow prior to the onset of t_d. In the present measurements, no voltage fluctuations or steps were detected prior to the appearance of the delayed voltage response; however, this observation alone does not exclude vortex-mediated dissipation, which may contribute after the onset of the resistive state. In the present measurements, no such signatures were observed before the delay time t_d, indicating that these mechanisms do not trigger the dissipation. This observation does not exclude the possible involvement of vortices after the onset of the resistive state. Our measurements were performed in the absence of a magnetic field, and the dissipation we observed was dominated by the hotspot (HS) mode. Using the electrical pulse technique, we induced non-equilibrium states that gave rise to a voltage response after a well-defined delay time t_d, associated with either PSC or HS formation. However, no vortex nucleation was observed before the delay time that would signal PSC dissipation.

The delay time t_d was analyzed within the framework of the TDGL, later refined by Tinkham [12], which provides the expression:

$$t_d(I/I_c) = \tau_d \int_0^1 \frac{2f^4 df}{\frac{4}{27}(\frac{I}{I_c})^2 - f^4 + f^6} \tag{1}$$

where f is the normalized order parameter, I is the applied current, and τ_d is a fitting parameter reflecting the characteristic relaxation time of the system.

The sample was first investigated under vacuum at T = 4.2 K. For currents exceeding I_c, after the delay time t_d a sudden, monotonic increase in voltage was observed across the sample, which we identify as the formation of a HS. This delay decreased systematically with increasing amplitude of the applied current. Figure 2 shows the measured values of t_d as a function of current, fitted with (1), yielding a characteristic parameter $\tau_d = 6.0 \pm 0.5$ ns.

Within the dissipative zone, the local temperature exceeds the substrate temperature [22]. Heat generated inside the hotspot is initially confined within a region bounded by superconducting zones on either side. Energy is then redistributed to the neighboring superconducting parts through quasi-particles (QP) and phonons, leading to the extension of the HS length, while a fraction of the heat is transferred to the substrate. The non-equilibrium system can thus be viewed as two coupled subsystems: QPs and phonons. The Rothwarf–Taylor (RT) model [23] describes the coupled time evolution of these subsystems. Once Cooper pairs are broken, the resulting QPs are excited to high-energy states. The rapid electron electron interactions are followed by slower electron phonon processes, after which QPs accumulate near the band edge at energies 2Δ above the gap. Finally, recombination of QPs occurs, releasing energy as phonons that carry heat to the substrate.

The same sample was then studied in liquid helium using the identical setup. Figure 3 shows the variation of the delay time t_d with current. Fitting with (1) yielded $\tau_d = 5.3 \pm 0.5$ ns, a value slightly smaller than that obtained under vacuum. This parameter reflects the effective cooling time of the film. Although the current and voltage amplitudes in both environments were nearly identical (difference less than 9%), the faster heat removal in liquid helium reduces τ_d. The additional cooling pathway is

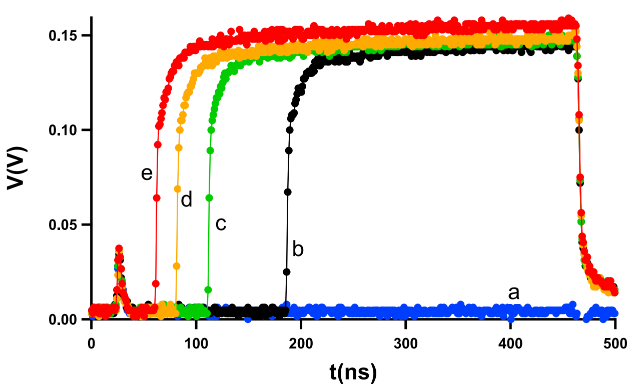

Fig. 2 Temporal evolution of the voltage generated by a single-step current pulse in the NbTi bridge immersed in liquid helium. The voltage shown corresponds to the signal measured at the upper lateral probe with respect to ground; no voltage signal is detected at the lower probe. The voltage appears only after a delay time t_d, and this delay decreases as the applied current increases. The traces correspond to I/I_c= 1, 1.008,1.025, 1.050 and 1.070 (labeled a to e, respectively)

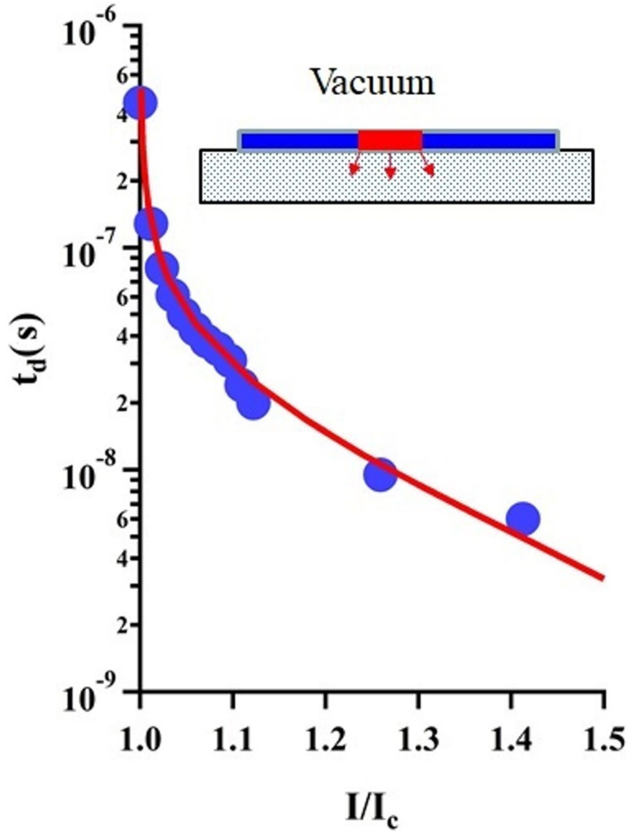

Fig. 3 Logarithmic scale of the delay time-current characteristics of 50 nm thick and 5 μm wide NbTi filament measured in vacuum (dots) at T = 4.2 K. The fitting curve (red) is the TDGL with a prefactor τ_d = 6.0 ± 0.5 ns

provided by direct heat exchange between the hotspot and the surrounding helium bath through the upper surface and lateral sides of the wire (Fig. 4).

The comparison between vacuum and liquid helium conditions emphasizes the role of the environment in determining the heat escape dynamics. In both cases, the dominant fraction of the heat is evacuated into the substrate. However, in liquid helium, the wire has an extra dissipation channel through the helium bath, which marginally reduces the overall heat escape time. The small difference between the measured τ_d values (6.0 ± 0.5 ns in vacuum and 5.3 ± 0.5 ns in liquid helium) demonstrates that while substrate cooling is the primary pathway, immersion in liquid helium introduces an additional but less dominant mechanism for heat evacuation.

4 Conclusion

Resistive states in superconducting thin NbTi wires were induced by electrical current pulses and investigated under two different thermal environments: vacuum and liquid

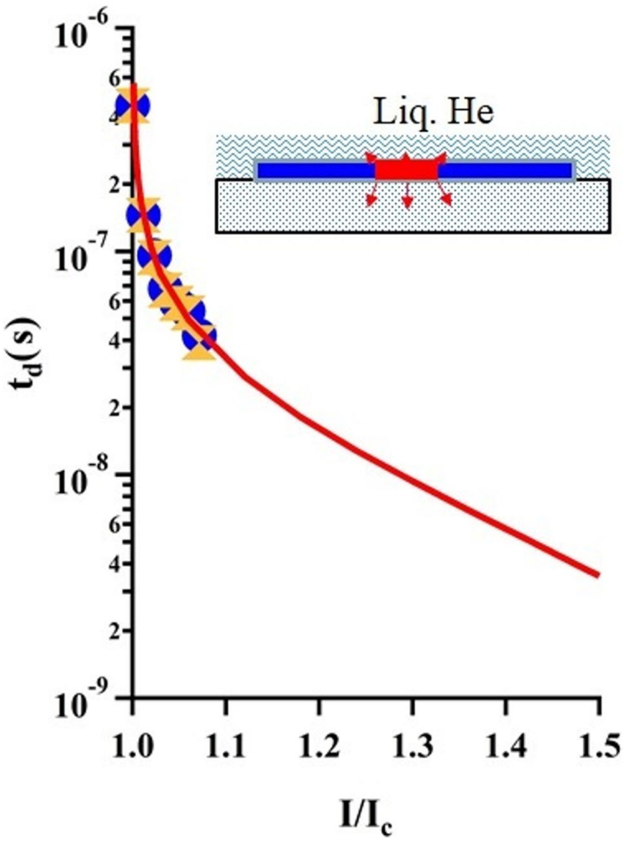

Fig. 4 The dependence of the delay time t_d on the reduced current I/I_c of NbTi filament submerged in liquid helium. The solid line is the best fit of the experimental results with the TDGL (1) with a prefactor τ_d = 5.3 ± 0.5 ns

helium. The resulting non-equilibrium dynamics were characterized by the delay time t_d, which was analyzed within the framework of the time-dependent Ginzburg–Landau (TDGL) model. From this analysis, effective heat escape times were extracted for both environments. The measured values differ by only about 9% between vacuum and liquid helium, indicating that heat dissipation is dominated by transfer into the substrate. While the observed behavior is consistent with hotspot-related dissipation, additional mechanisms such as vortex dynamics may also contribute to the resistive response, particularly after the onset of dissipation. The comparatively small influence of the liquid helium environment suggests that substrate coupling plays the primary role in governing the thermal relaxation processes in the NbTi films.

Acknowledgements K.H. gratefully acknowledges the support of King Fahd University of Petroleum and Minerals, Saudi Arabia, under project INSS2504. The assistance of A.I. was utilized for English polishing of this manuscript.

Author Contributions K.H. carried out the experiments, performed the data analysis, and contributed to the writing and revision of the manuscript.

Data Availability No datasets were generated or analysed during the current study.

Declarations

Competing Interests The authors declare no competing interests.

References

1. Zhang, L., You, L., et al.: Sci. Rep. **8**, 1486 (2018)
2. Baumans, X.D.A., et al.: Sci. Rep. **7**, 44569 (2017)
3. Buh, J., Kabanov, V., Baranov, V., Mrzel1, A., Kovic, A., Mihailovic, D.: Nat. Commun. **6**, 10250 (2015)
4. Chen, Y., Lin, Y.-H., Snyder, S.D., Goldman, A.M., Kamenev, A.: Nat. Phys. **10**, 567–571 (2014)
5. Zhao, Q.Y., et al.: Nat. Photonics **11**, 247 (2017)
6. Madan, I., Buh, J., Baranov, V.V., Kabanov, V.V., Mrzel, A., Mihailovic, D.: Sci. Adv. **4**, eaao0043 (2018)
7. Zhang, H., Xiao, L., Luo, B., Guo, J., Zhang, L., Xie, J.: J. Phys. D Appl. Phys. **53**, 013001 (2020)
8. McCaughan, A.N.: Supercond. Sci. Technol. **31**, 040501 (2018)
9. Mooij, J.E., Nazarov, Y.V.: Nat. Phys. **2**, 169 (2006)
10. Astafiev, O.V., Ioffe, L.B., Kafanov, S., Pashkin, Y.A., Arutyunov, K.Y., Shahar, D., Cohen, O., Tsai, J.S.: Nature **484**, 355 (2012)
11. Tinkham, M.: Intro. to Superconductivity, 2nd ed. (McGraw-Hill, Singapore), Chap 11 (1996)
12. Tinkham, M.: in Non-Equilibrium Superconductivity, Phonons and Kapitza Boundaries, K.E. Gray (ed.), (Plenum, New York), pp. 231–262 (1981)
13. Harrabi, K.: Appl. Phys. A **125**, 751 (2019)
14. Yu, D., Vodolazov, F.M. Peeters: Phys. Rev. B **90**, 094504 (2014)
15. Skocpol, W.J., Beasley, M.R., Tinkham, M.: J. Appl. Phys. **45**, 4054 (1974)
16. Berdiyorov, G., Harrabi, K., Oktasendra, F., Gasmi, K., Mansour, A.I., Maneval, J.P., Peeters, F.M.: Phys. Rev. B **90**, 054506 (2014)
17. Sivakov, A.G., et al.: Phys. Rev. Lett. **91**, 267001 (2003)
18. Weber, A., Kramer, L.: J. Low Temp. Phys. **84**, 289 (1991)
19. Andronov, A., Gordion, I., Kurin, V.: Nefedov I and Shereshevsky IPhysica C **213**, 193–9 (1993)
20. Paradiso, N., Nguyen, A.T., Kloss, K.E., Strunk, C.: 2D Mater. **6**, 025039 (2019)
21. Dmitriev, V.M., Zolochevskii, I.V., Salenkova, T.V., Khristenko, E.V.: Low Temp. Phys. **31**, 127–36 (2005)
22. Harrabi, K., Mekki, A., Bahlouli, H., Mathieu, P.: Mater. Res. Express **8**, 056001 (2021)
23. Rothwarf, A., Taylor, B.N.: Phys. Rev. Lett. **19**, 27 (1967)